IEEE Access
Multidisciplinary | Rapid Review | Open Access Journal

Received January 17, 2019, accepted January 23, 2019, date of publication January 31, 2019, date of current version February 20, 2019.

Digital Object Identifier 10.1109/ACCESS.2019.2896640

Low Detection Limit Time-Correlated Single Photon Counting Lifetime Analytical System for Point-of-Care Applications

YI TIAN, WENRONG YAN, LIPING WEI, AND DEREK HO, (Member, IEEE)
Department of Materials Science and Engineering, City University of Hong Kong, Hong Kong

Corresponding author: Derek Ho (derekho@cityu.edu.hk)

This work was supported in part by the Hong Kong Research Grants Council under Grant 11213515.

ABSTRACT Photon-counting analysis plays a key role in many areas, such as biology, chemistry, and medicine. In this paper, we present an integrated time-correlated single photon counting (TCSPC) lifetime analytical system with a complete signal path—from fluorophore excitation, emission detection, to lifetime extraction. The time-to-digital module of the proposed TCSPC system achieves a root-mean-square differential non-linearity of 4% of the least significant bit and a full width at half maximum temporal resolution from 121 to 145 ps within the 500-ns full-scale range. To evaluate the lifetime extraction and detection limit of the proposed TCSPC system, a wide variety of samples, such as fluorescein in water, coumarin 6 in dimethyl sulfoxide, and rhodamine 6G in water, each prepared in 14 concentrations from 0.5 nM (nanomolar, 10^{-9} mol/L) to 25 μM (micromolar, 10^{-6} mol/L), are tested. With the optimized hardware and firmware design, the proposed TCSPC system can accurately extract the fluorescence lifetime of fluorescein, coumarin 6, and rhodamine 6G down to the concentration of 1, 1, and 2.5 nM, respectively, significantly outperforming similar fluorescence lifetime analysis systems.

INDEX TERMS Non-invasive optical analysis, time-correlated single photon counting, low detection limit, fluorescence lifetime extraction.

I. INTRODUCTION

Fluorescence analysis has become an increasingly well-adopted technique in analytical chemistry, medical diagnostics, and biological research, recently many research works have been proposed to related areas [1]–[10]. As fluorescence analytical instruments are usually implemented in the compact system scale, it becomes increasingly difficult to provide good excitation rejection. The large background noise degrades signal to noise performance. Recently, lifetime techniques have gained wide interest as a way to address the above limitation, predicated on the fact that detection is typically performed when the pulsed excitation is in the off state. In addition, the lifetime of a fluorescence molecule is sensitive and specific to the surrounding chemical environment, rendering lifetime techniques selective analytical methods [11].

Fluorescent samples such as Fluorescein [12]–[16], Coumarin 6 [17]–[20] and Rhodamine 6G [21]–[25] have been used widely as biomarkers. For many *in vivo* experiments, increasing the concentration of fluorescent probes can precipitate molecules, cause cellular distortions, self-quenching, or induce cell death. Therefore, a low detection limit, which is defined as the lowest analyte concentration that the instrument can reliably obtain the fluorescence lifetime [26], is required in many fluorescence analysis experiments. Designing a compact, portable, and integrated system for sensing chemical and biological samples with a detection limit lower than those of conventional fluorescence lifetime analysis systems is the target of this work.

Fluorescence lifetime analysis techniques can be classified into frequency-domain and time-domain techniques. Frequency-domain techniques record the phase and amplitude of the signal as a function of frequency whereas time-domain techniques record the intensity of the signal as a function of time [27]. These two techniques require different hardware architectures resulting in different performance, suitable for various applications.

Using frequency domain techniques, fluorescence lifetimes can be determined by a phase-modulation technique.

The associate editor coordinating the review of this manuscript and approving it for publication was Xiao-Sheng Si.

A modulated light source is used to excite the fluorescent sample. The resulting emission signal from the sample has a similar but modulated and phase-shifted waveform in comparison to the excitation signal. Both characteristic modulation and phase-shift are determined by the lifetime of the fluorescence emission, therefore lifetime can be calculated from the observed modulation and phase-shift [28]. The frequency-domain fluorescence lifetime analysis techniques are compatible with tunable continuous-wave excitation source that seamlessly covers a wide spectral range. However, under weak photon emission from the sample, the accuracy of fluorescence lifetime detection is severely degraded.

Time domain techniques can generally be subdivided into time-gated photon counting and time-correlated single photon counting (TCSPC) [29]. Time-gated photon counting is used in combination with laser scanning to record fluorescence lifetime information at high efficiency. Time-gated technique operates on a timescale orders of magnitude greater than frequency domain methods [30]. The time-gated detector can reject most of the early arrival emitted photons [31], thus greatly reducing the amount of unfiltered excitation photons detected by the detector. However, the amplitudes and lifetime parameters of multiexponential decay profiles are difficult to obtain [32]. Moreover, the temporal resolution of existing time-gated photon counting implementations is generally limited. For instance, the histogram temporal resolution of time-resolved fluorescence analysis microsystem [33] and portable time-domain LED fluorimeter [34] are 450 ps and 250 ps, respectively, which are insufficient and can influence the accuracy of the lifetime measurements. This can be improved by using TCSPC.

With the advance of integrated electronics, TCSPC has been recently applied to fluorescence correlation spectroscopy [35], fluorescence lifetime imaging (FLIM), fluorescence resonance energy transfer (FRET) [11], [32], [36], [37], and other applications due to its high temporal resolution, high sensitivity, high counting efficiency, high signal-to-noise ratio (SNR) [38] and short measurement time. TCSPC measures the elapsed time between an excitation pulse (START) and the corresponding emission fluorescence photon arrival (STOP) repetitively with sub-nanosecond temporal resolution. After the detection of several photons, a histogram whose x-axis represents the elapsed time delay and y-axis represents the number of photons collected for each time delay is built. The shape of the histogram represents the optical signal emitted by the excited sample [39] and the lifetime of the fluorescence emission can be extracted from the histogram. The histogramming process avoids any time gating or wavelength scanning, thus yielding a better counting efficiency than the time-gated photon counting technique [37].

In terms of system building blocks, much work has been done to develop high-performance time-to-digital converters (TDCs) [40]–[44] or time-gated detectors [31], [45]–[48] and single-photon avalanche diodes (SPADs) [49], [50] recently. Also, photon counting systems for non-invasive fluorescence lifetime analysis have been proposed albeit with relatively low level of integration [5], [28], [34], [39], [51]–[56], but most of these designs neither present a convenient way to extract fluorescence lifetime nor verify the accuracy of the fluorescence lifetime measurement. There are also chip-level implementations of fluorescence lifetime measurement systems [33], [57], [58] with a high-level of integration and generally low power consumption. However, fluorescence lifetime measurements tend to be of low to medium volume applications, where discrete implementation has the advantage of a short production cycle, low startup cost, and large flexibility in implementing design revisions. Therefore, further improvements to discrete implementations of lifetime analytical systems combining data-acquisition with lifetime extraction is of great demand.

In this paper, we present a compact, low detection limit TCSPC system with fluorescence lifetime extraction. By using a digital TDC to sample and digitalize the elapsed time between excitation and emission, the system achieves a temporal resolution from 121 ps to 145 ps within the FSR of 500 ns for time-to-digital measurements. The conversion speed of the proposed TCSPC system is up to 160k samples per second (sps). Fluorescence lifetime extraction is achieved by employing the non-linear least square (NLLS) method [59]–[61] and experimentally demonstrated using different fluorescent samples. The detection limit is evaluated by Fluorescein in water, Coumarin 6 in Dimethyl sulfoxide (DMSO), and Rhodamine 6G in water, each prepared in 14 concentrations, from 0.5 nM (nanomolar, 10^{-9} mol/L) to 25 μM (micromolar, 10^{-6} mol/L), in order to introduce minimum influence of *in vivo* experiments. The proposed TCSPC system can accurately extract lifetime of Fluorescein in water, Coumarin 6 in DMSO and Rhodamine 6G in water down to the concentration of 1 nM, 1 nM, and 2.5 nM, respectively, significantly outperforming similar fluorescence lifetime analysis systems in terms of detection limit.

This paper is organized as follows. Section II discusses the theory of fluorescence lifetime extraction. Section III, IV, and V present the system architecture and implementation and experimental results, respectively. Section VI concludes the paper.

II. THEORY

Upon the removal of optical excitation from a fluorescence molecule, the emission typically follows a decaying profile, which is often fitted by negative multi-exponential functions [62]. Fluorescence lifetimes are the time constants of the multi-exponential decay. Therefore, the theoretical fluorescence decay $F(t)$ as a function of time t is conventionally described by the multi-exponential equation [11], [38], given by

$$F(t) = \sum_{j=1}^{m} \alpha_j \exp(-t/\tau_j) \tag{1}$$

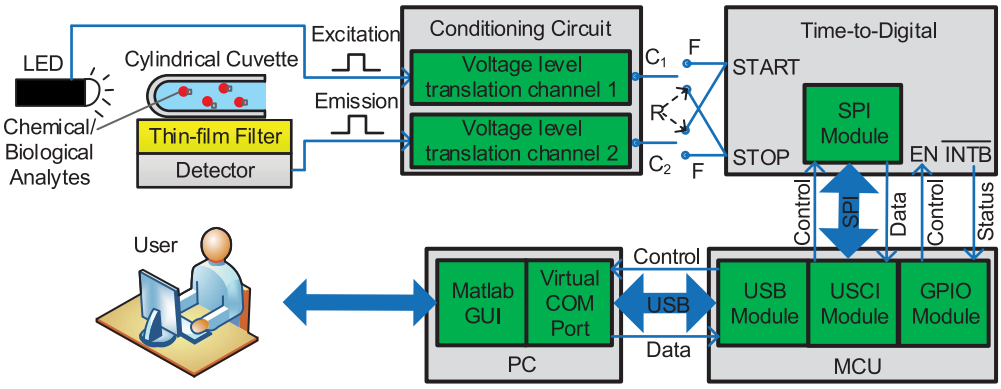

FIGURE 1. Architectural block diagram of the proposed TCSPC system.

where m is the number of fluorescence lifetime components, α_j and τ_j are the decay amplitude and fluorescence lifetime of the j'th component, respectively. Fluorescence lifetime τ is defined as the time when fluorescence intensity attenuates to $1/e$ of the initial intensity for a single exponential decay ($m = 1$) [63]. An accurate fluorescence lifetime measurement normally requires the instrument response function (IRF), $h(t)$, which is measured using a reference sample that directs a small fraction of the excitation light into the detection path in advance. Then the measured fluorescence decay $R(t)$ is measured when the reference sample is replaced by the fluorescent sample. $R(t)$ contains the instrumental effect and is given by the convolution of $F(t)$ with $h(t)$ [11], [38], given by

$$R(t) = F(t) \otimes h(t) \tag{2}$$

Therefore, the theoretical fluorescence decay $F(t)$ is then obtained by the deconvolution of the measured fluorescence decay and the IRF [27], [64].

NLLS has been one of the most commonly used methods recently for the analysis of TCSPC data to estimate decay amplitude and fluorescence lifetime [65]. Therefore, it is employed in the proposed TCSPC system to extract lifetime of measured fluorescent samples. NLLS is achieved by evaluating the goodness-of-fit from the reduced chi-square error, given by

$$\chi_r^2(t) = \frac{1}{a-b} \sum_{i=1}^{n} \frac{[R(t_i) - R_c(t_i)]^2}{\sigma_i^2} \tag{3}$$

where a is the number of data points, b is the number of estimated parameters, and σ_i is the standard deviation of the photon count in the i'th time bin [11], [38], [66]. A good fit is characterized by a value of $\chi_r^2(t)$ close to 1. The residual between the measured and calculated decay curve should be randomly distributed around 0. For example, Preus [67] uses a simplex search method of Lagarias *et al.* [68] that successively minimizes the error $\chi_r^2(t)$.

III. SYSTEM ARCHITECTURE

The architectural block diagram of the proposed TCSPC system is shown in Fig. 1. A pulsed excitation light emitting diode (LED) excites the fluorescent analytes in a cylindrical cuvette. Due to Stokes' shift, the emitted photons have longer wavelengths than that of the excitation. With a thin-film filter filtering out the excitation photons, the emitted photons can be detected by the photon detector. The pulse signals of both the excitation source and the detector constitute a signal pair of the proposed TCSPC system. The system can be divided into four blocks, including micro-optics, time-to-digital module with signal conditioning circuit, microcontroller unit (MCU) and graphical user interface (GUI).

IV. IMPLEMENTATION

Fig. 2 depicts top view and side view of the proposed TCSPC system. The system consists of a 35 mm diameter NanoLED excitation source and four stacked printed circuit boards (from top to bottom: detector, time-to-digital module, MCU and conditioning circuit). The sample is held in a cylindrical cuvette to be excited and analyzed. The pulse signals of excitation and emission are transmitted by coaxial cables via SMA connectors and a USB cable provides communication to a PC.

A. EXCITATION FILTERING AND OPTICAL CONSIDERATIONS

In a practical TCSPC system using a thin-film filter, excitation rejection is inadequate, thus, both emission and a portion of the excitation reach the detector. Therefore, the total number of photons reaching the detector active area N_{tot} is given by

$$N_{tot} = N_{ex} + N_{em} \tag{4}$$

where N_{ex} and N_{em} are the numbers of unfiltered excitation and emitted photons reaching the detector, respectively. The relative emission intensity η_{em} can be defined as

$$\eta_{em} = N_{em}/N_{tot} \tag{5}$$

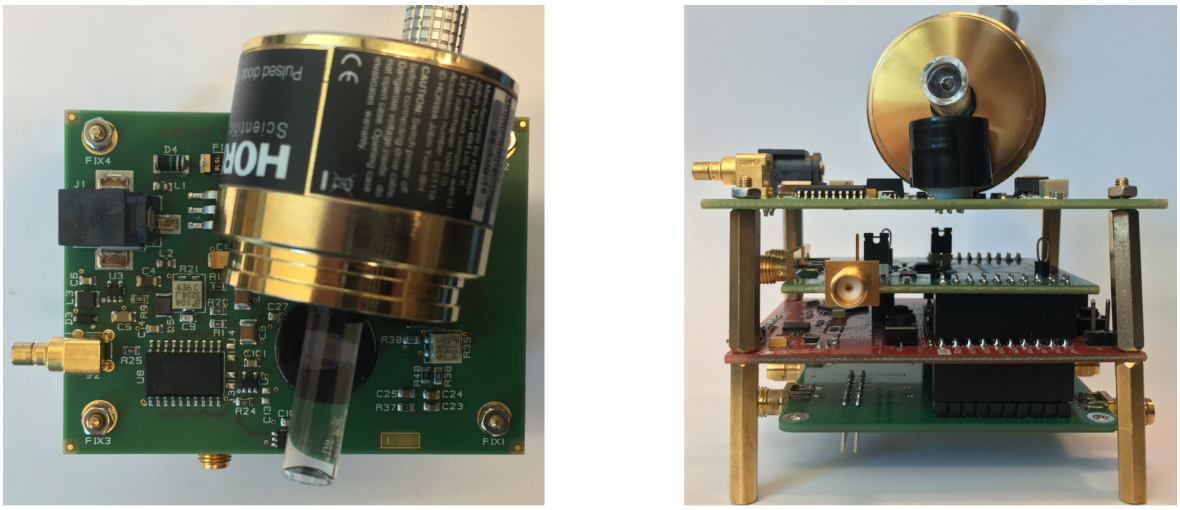

(a) (b)

FIGURE 2. (a) Top view and (b) side view of the proposed TCSPC system when an SPAD is selected as the detector with the size of 73.5 mm (L) × 61.3 mm (W) × 92.6 mm (H) (without cables). The pulse signals of excitation and emission are transmitted by coaxial cables via SMA connectors. An USB cable connecting to PC is used for both communication and power supply.

According to the Beer-Lambert Law [69], N_{em} decreases with a reduction in the concentration of fluorescent sample. Therefore, as η_{em} reduces, the background caused by unfiltered excitation photons becomes significant, making the fluorescence lifetime difficult to extract.

Another phenomenon that influences lifetime extraction is photobleaching, a photochemical alteration caused by prolonged excitation of fluorescent molecules, a.k.a fluorophores or dyes, leading to an eventual loss of their capacity to fluoresce [70]. Prolonged measurement not only reduces the emission intensity but also heats the electronic components of the system. Both the reduced emission intensity due to photobleaching and drift due to electronic components heating degrade the sensitivity of the system. Therefore, the proposed TCSPC system needs to be designed to increase conversion rate and to decrease the influence of temperature, key factors for achieving a low detection limit.

B. EXCITATION SOURCE

TCSPC applications require a pulsed excitation source at the wavelength from the UV to blue as many organic dyes and quantum dots absorb light most efficiently at this wavelength range. UV is even better than blue for many probes, but UV has been shown to damage or harm biological samples [71]. Therefore, a pulsed excitation in the violet-blue spectral range is selected for the proposed TCSPC system.

The HORIBA NanoLED N-455 light source, a nanosecond LED with a pulse full width at half maximum (FWHM) of 1.3 ns, 455 ± 10 nm peak wavelength, 7 pJ per pulse energy, a maximum repetition rate of 1 MHz is driven by a dedicated driver integrated circuit. The output pulse signal is selectable between NIM-compatible (Vpp = −0.8 V) and TTL-compatible (Vpp = +2 V). All these features make NanoLED a suitable choice for compact fluorescence lifetime measurements.

C. DETECTOR

Photomultiplier tubes (PMTs) and SPADs are the most widely used photon counting detection technologies to-date [72]. The proposed TCSPC system is designed to be compatible with both detectors, rendering the system suitable for a variety of applications. Therefore, a PMT and an SPAD are selected as the alternative detector of the proposed TCSPC system.

1) PMT

The HORIBA PPD 650 picosecond photon detection module featuring < 0.25 ns risetime PMT is chosen. The 8mm diameter PMT covers the spectral range between 230 and 700 nm, and the maximum detection efficiency reaches around 35% between 300 and 500 nm. With a less than 80 counts per second (cps) dark count rate, 125 ps temporal resolution, and selectable output pulse signal between NIM and TTL, the HORIBA PPD 650 is suitable for accurate fluorescence lifetime measurements.

2) SPAD

The IDQ ID101-50 CMOS silicon chip combining a 50μm diameter single SPAD and an active quenching circuit with less than 50 ns deadtime is selected as an alternative detector. The SPAD covers the spectral range between 350 and 900 nm, and the maximum detection efficiency is measured to be 35% at 500 nm. With 100 cps dark count rate, 40 ps temporal resolution, 0.5% afterpulsing probability, and an output pulse signal of +5V Vpp, The IDQ ID101-50 is suitable for compact fluorescence lifetime applications.

3) TRADE-OFF

PMTs offer large active area (up to cm^2), no dead time, the ability to record low dark current (down to 10^{-8} A/cm^2) at no added cost, and negligible thermal noise of the load resistance respect to the quantum noise that the detected current already carries. But PMTs are relatively bulky and fragile components, difficult to be qualified for use in demanding environment such as space, nuclear, and high electromagnetic interference (EMI) [73]. On the other hand, SPADs have easy compatibility to the standard CMOS process, reduced junction transit time and jitter of the pulse response, and the capability to be unaffected by strong electromagnetic fields [74]. However, SPADs have a dead time following each detected event [73], typically stronger afterpulsing probability than in PMTs increasing the noise background, and smaller active area compared to PMTs decreasing the collection efficiency when the optical signal arises from a large area and wide emitting angle [75]. Therefore, PMTs or SPADs can be chosen according to the requirements of different TCSPC lifetime applications. In measurements that require portability, an SPAD can be chosen as the detector. When the optical signal is relatively weak, to obtain a sufficiently high SNR for good lifetime extraction accuracy, a PMT can be selected at the expense of bulkiness.

As depicted in Fig. 2, when an SPAD is selected as the detector, the size of the proposed TCSPC system is 73.5 mm (L) × 61.3 mm (W) × 92.6 mm (H). When a PMT is selected, the detector board with SPAD is replaced by a PMT mounted on the chassis, thus increasing the system size slightly to 107.5 mm (L) × 76.8 mm (W) × 136.2 mm (H).

D. TIME-TO-DIGITAL MODULE WITH SIGNAL CONDITIONING CIRCUIT

Time-to-digital module of TCSPC applications requires conversion with reliable pico-second temporal resolution. The Texas Instruments time-to-digital converter TDC7200 is selected to convert elapsed time between the input signal pair to digital values because of its temporal resolution, self-calibration and insensitivity to temperature. TDC7200 is a stopwatch integrated circuit with 55 ps least significant bit (LSB) resolution used to measure the elapsed time between a single event (an edge on START pin) and multiple subsequent events (an edge on STOP pin). An internal self-calibrated timer base inside TDC7200 compensates for drift over time and temperature. All these features make the TDC7200 specifically suitable for TCSPC lifetime measurement. The completion interrupt status of time-to-digital conversion is continuously checked by the MCU during the measurement. When a time-to-digital conversion has completed, the result is read into the MCU and the next conversion is initiated.

Since the output high voltages of the excitation source and the alternative detectors are not compatible with the TDC7200, a signal conditioning circuit with Texas Instruments LSF0102 two-channel bidirectional multi-voltage translator is designed as the interface between the input signal pair and the TDC module to satisfy signal compatibility. As depicted in Fig. 1, connectors C1, C2 between the signal conditioning circuit and time-to-digital module can be switched between "F" and "R" position to conduct TCSPC measurement in forward or reverse START-STOP mode.

E. MCU

The Texas Instruments low-power MCU MSP430F5529 is selected as the core controller of the system. The MCU also processes the TCSPC signals and relay data/user commands to/from the PC. After system initialization, the MCU continuously polls for START commands sent from the user, then controls the TDC7200 to obtain the elapsed time between the input signal pair. The conversion results within the user customized measurement range are considered valid, thus stored in the MCU before transmitting to the PC for further analysis. Upon receiving the STOP command, the MCU terminates the time-to-digital conversion, then lifetime extraction is performed. Approximately 2.7 seconds are required to extract the lifetime of 3.0×10^7 valid conversion results on a 2.27 GHz dual core CPU. By only keeping the valid conversion results, the system can achieve valid conversions up to 160k sps, which enables the system to achieve a low detection limit.

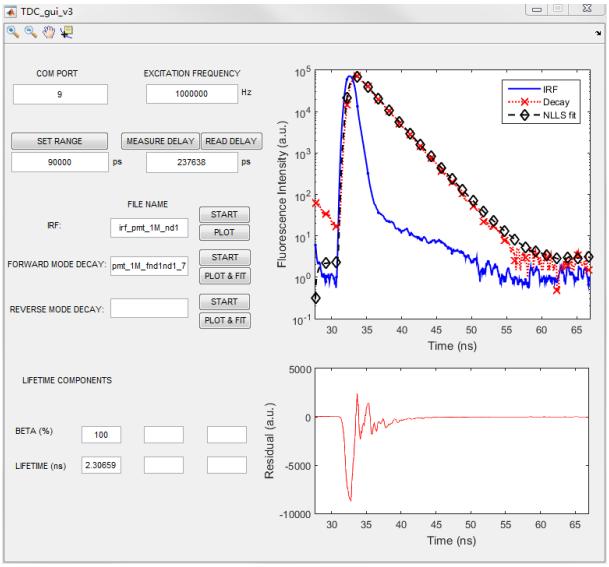

FIGURE 3. Customized GUI on PC.

F. GRAPHICAL USER INTERFACE

For user convenience, the top-level system control is performed by a customized GUI, as shown in Fig. 3. The MATLAB script opens the communication through a virtual serial port via USB and sends out the control commands to trigger the configured measurement. During the measurement, conversion results are received through multiple packages via USB. Once the measurement is terminated by the user, all digitalized elapsed time data are

saved into a file, with which fluorescence lifetime is subsequently extracted using NLLS method. Lifetime extraction has been implemented as post-processing computation to add flexibility in performance optimization of the system. In fact, the employed NLLS is a commonly used method for fluorescence lifetime extraction and has been shown to be readily implemented on the MCU and other embedded hardware [76], [77]. The measured IRF curve, fluorescence decay curve, NLLS fitting curve and the extracted fluorescence lifetime are displayed on the GUI. With a customized, user-friendly GUI, the TCSPC system can be conveniently controlled and operated.

V. EXPERIMENTAL RESULTS

Several tests are made to evaluate the performance of the proposed TCSPC system in terms of differential non-linearity (DNL), FWHM temporal resolution of the TDC module, and lifetime extraction, detection limit of the system.

A. DNL

1) SETUP

The DNL of TDC module of the proposed TCSPC system is assessed through the code density test. The employed setup consists of two pulse generators: one providing the STOP signal with a fixed rate and the other generates a random signal used as the START signal, where the START and STOP signals are uncorrelated [39], [53]. The code density test shows a distribution that reflects both the DNL of the system and the statistical noise of the input signal. Therefore, to have a reasonably flat START-STOP input signal distribution, at least 10K conversion results per histogram bin are needed to achieve a $<1\%$ statistical noise [5], [78].

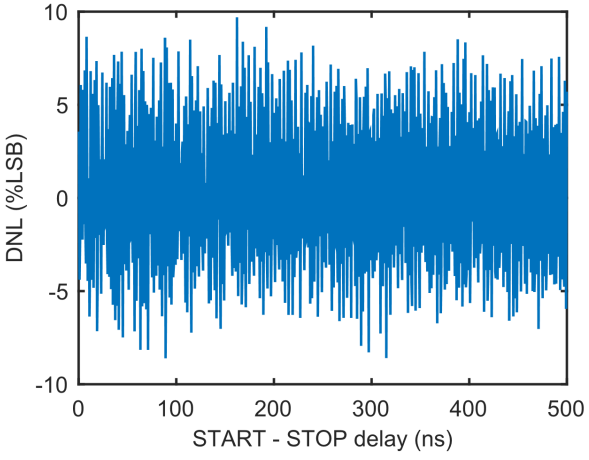

FIGURE 4. Measured DNL of TDC module of the proposed TCSPC system.

2) RESULT

The measured distribution of the code density test is shown in Fig. 4, ranging between $+9.7\%$ and -8.5% of the LSB, with an average root mean square (RMS) value of 4% of LSB within the 500 ns FSR. The average results per histogram bin are 3×10^4, thus the statistical noise of signal distribution is 0.6%, which is negligible in relation to the overall distribution.

B. FWHM TEMPORAL RESOLUTION

1) SETUP

The temporal resolution of TDC module of the proposed TCSPC system is characterized by the FWHM of the response to a given time interval event [79]. To measure the FWHM temporal resolution, START-STOP signal pair is obtained by splitting the output of a pulse generator. A fixed START-STOP delay can be obtained by using a passive adjustable delay line along the STOP signal path in order not to introduce additional jitter.

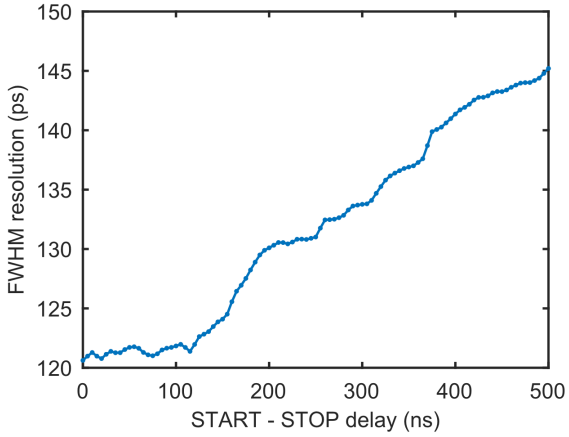

FIGURE 5. Measued FWHM temporal resolution of TDC module of the proposed TCSPC system.

2) RESULT

As depicted in Fig. 5, the measured FWHM temporal resolution of TDC module of the proposed TCSPC system is about 121 ps in the first 121 ns of the FSR and then it starts to worsen, reaching 145 ps at the end of the 500 ns FSR. The worsening in FWHM temporal resolution at longer START-STOP delays is mainly caused by the superposition of non-linearity of delay elements inside the TDC7200 for longer START-STOP delays.

C. LIFETIME EXTRACTION

1) SETUP

The lifetime extraction performance of the proposed TCSPC system is experimentally validated by testing with 3 commercially available fluorescent samples, including Fluorescein (Sigma-Aldrich) in water, Rhodamine 6G (Shanghai Gold Wheat) in water and Coumarin 6 (Sigma-Aldrich) in DMSO. During the measurement, de-ionized water is used as a reference to acquire the IRF of the proposed TCSPC system, then de-ionized water is replaced with the testing fluorescent sample to measure the decay curve.

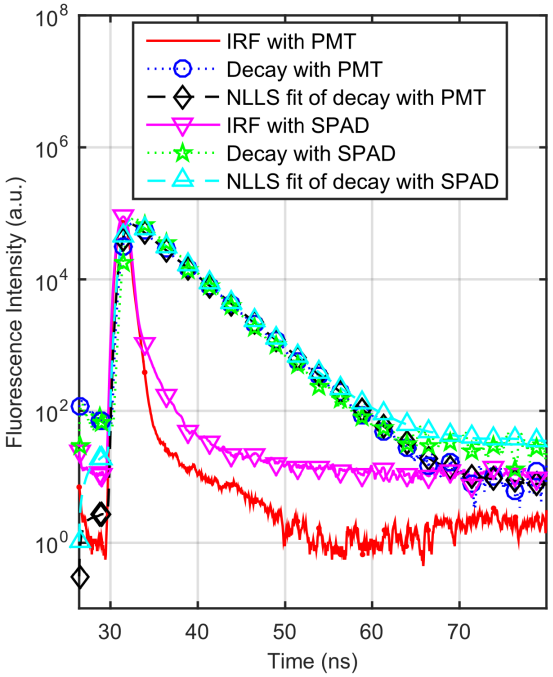

FIGURE 6. IRF and fluorescence decay of Fluorescein in water (5 μM) measured by the proposed TCSPC system plotted in semilog axis. Extracted fluorescence lifetimes of Fluorescein in water with PMT and SPAD are 3.99 ns and 4.09 ns, respectively, compared to the specification value of 4.00 ns.

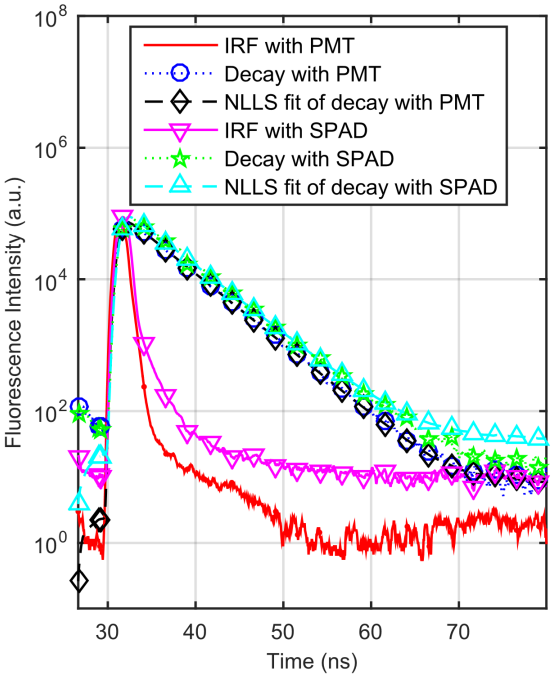

FIGURE 7. IRF and fluorescence decay of Rhodamine 6G in water (5 μM) measured by the proposed TCSPC system plotted in semilog axis. Extracted fluorescence lifetime of Rhodamine 6G in water with PMT and SPAD are 4.04 ns and 4.07 ns, respectively, compared to the specification value of 4.0 ns.

2) RESULT

Fig. 6 shows the measured IRF of TCSPC system and the decay curve of Fluorescein in water (5 μM). The FWHM of IRF is 1.35 ns and extracted fluorescence lifetime of Fluorescein in water with PMT and SPAD are 3.99 ns and 4.09 ns, respectively, compared to the specification value of 4.00 ns. Based on the same measurement protocol, two other commercial fluorescent samples are also measured as plotted in Fig. 7 and Fig. 8. The extracted fluorescence lifetime of Rhodamine 6G in water (5 μM) with PMT and SPAD are 4.04 ns and 4.07 ns, respectively, compared to the specification value of 4.00 ns. The extracted fluorescence lifetime of Coumarin 6 in DMSO (5 μM) with PMT and SPAD are 2.32 ns and 2.45 ns, respectively, compared to the specification value of 2.32 ns [80]. These results show that the proposed TCSPC system can extract lifetime of different fluorescent samples accurately.

D. DETECTION LIMIT

1) SETUP

In order to evaluate the detection limit of the proposed TCSPC system with PMT (SPAD) and compare it with similar fluorescence lifetime analysis systems [26], [28], [33], [34], [55], each of Fluorescein in water, Coumarin 6 in DMSO and Rhodamine 6G in water is prepared in 14 concentrations (from 0.5 nM to 25 μM) and measured for 8 times with fluorescence lifetime separately extracted. Then, average value $\bar{\tau}$ and standard deviation σ of the extracted fluorescence lifetimes for each sample in 14 concentrations are calculated.

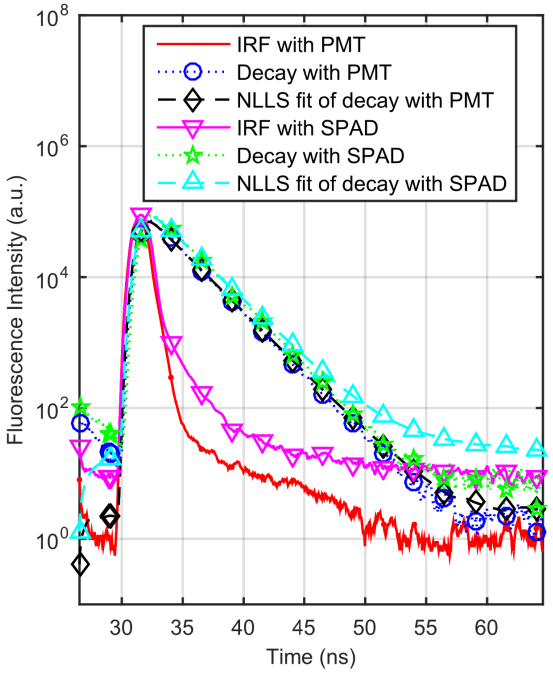

FIGURE 8. IRF and fluorescence decay of Coumarin 6 in DMSO (5 μM) measured by the proposed TCSPC system plotted in semilog axis. Extracted fluorescence lifetime of Coumarin 6 in DMSO with PMT and SPAD are 2.32 ns and 2.45 ns, respectively, compared to the specification value of 2.32 ns.

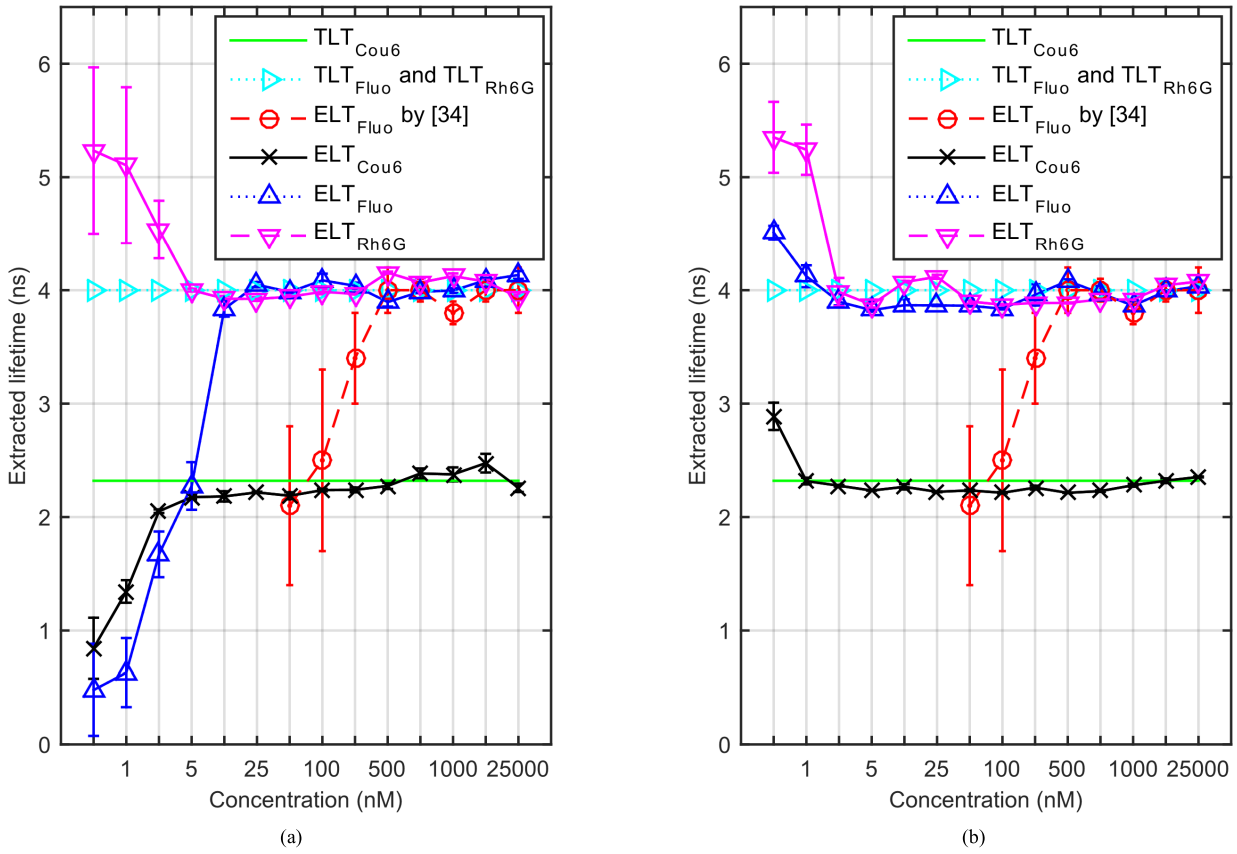

FIGURE 9. The statistical properties of the extracted lifetimes (ELTs) of the proposed TCSPC system with (a) SPAD and (b) PMT, and the theoretical lifetimes (TLTs) are also illustrated. Each of Fluorescein (Fluo) in water, Rhodamine 6G (Rh6G) in water, and Coumarin 6 (Cou6) in DMSO is prepared in 14 concentrations (0.5 nM, 1 nM, 2.5 nM, 5 nM, 10 nM, 25 nM, 50 nM, 100 nM, 250 nM, 500 nM, 750 nM, 1 μM, 5 μM, and 25 μM, respectively) and measured 8 times with fluorescence lifetime separately extracted. Then these data are used to calculate statistics, such as average fluorescence lifetime $\bar{\tau}$ and the standard deviation σ, and as a reference compared against time-gated fluorimeter of [34]. The detection limits of the proposed TCSPC system with PMT (SPAD) for Fluorescein in water, Coumarin 6 in DMSO and Rhodamine 6G in water are 1 nM (10 nM), 1 nM (5 nM) and 2.5 nM (5 nM), respectively. For samples having a concentration lower than the detection limit, the extracted fluorescence lifetime deviates from the factory-characterized value by greater than 5%. Whereas, for concentrations within the range of the system, it consistently provides extracted lifetime values that matches well with the reported value.

2) RESULT

The statistical properties of the extracted lifetimes of the proposed TCSPC system are shown in Fig. 9. The data suggest that the detection limits of the proposed TCSPC system with PMT(SPAD) for Fluorescein in water, Coumarin 6 in DMSO and Rhodamine 6G in water are 1 nM (10 nM), 1 nM (5 nM) and 2.5 nM (5 nM), respectively. When the samples are diluted less than the detection limits, the extracted fluorescence lifetime, e.g. the average value, begins to deviate from the specification value, with increased measurement variability.

The detection limit, error at detection limit, standard deviation at detection limit, number of channels, power consumption, and size of fluorescence lifetime analysis systems are compared in Table 1. The statistical properties of time-domain fluorimeter presented by Wang *et al.* [34] are also illustrated both in Fig. 9 and Table I with 0.5 μM detection limit for Fluorescein in water. The detection limit for CdSe/ZnS quantum dot samples of vertically integrated CMOS microsystem for time-resolved fluorescence analysis presented by Rae *et al.* [33], [55] is 0.01 μM. Portable phase fluorometer designed by Kissinger and Wilson [28] can extract fluorescence lifetime of Fluorescein in water down to the concentration of 7.5 μM. The lowest concentration experimentally injected for reliable lifetime measurement of Fluorescein in water is 1 nM for phase-sensitive fluorescence lifetime detection presented by He and Geng [26]. However, the deviation of the extracted fluorescent lifetime is greater than 5% and the standard deviation is larger than that of the proposed TCSPC system with PMT when the sample concentration is 1 nM. Therefore, the proposed TCSPC system significantly outperforms similar fluorescence lifetime analysis systems based on either time-gated photon counting or phase-modulated technique in terms of detection limit.

E. DISCUSSION

Experimental characterizations of lifetime extraction and detection limit show that the system performs better when a PMT is selected as the detector. The reason is that the PMT has a larger active area than the SPAD, thus obtaining

TABLE 1. Comparison table of fluorescence lifetime analysis systems in terms of detection limit.

System	This work[a]	This work[b]	H. Wang *et al.* [34]	B. R. Rae *et al.* [33], [55]	J. Kissinger *et al.* [28]	Y. He *et al.* [26]
Detection Limit	1 nM	5 nM	0.5 μM	0.01 μM	7.5 μM	1nM
Error at detection limit/Theoretical value (%)	3	6.2	0	N/A	N/A	6.25
Standard deviation at detection limit/Theoretical value (%)	2.4	0.9	5	N/A	N/A	5.75
Number of channels	1	1	1	64	1	1
Power consumption	Medium	Medium	Medium	Small	Small	N/A
Size	Medium	Medium	Medium	Small	Small	N/A

[a]For Fluorescein in water when a PMT is selected as the detector.
[b]For Coumarin 6 in DMSO when an SPAD is selected as the detector.

a better SNR. This accuracy-size trade-off is elaborated in Section IV.C.3. Nonetheless, the performance achievable by the SPAD is also sufficient for a variety of practical applications.

VI. CONCLUSION

In this paper, a low detection limit TCSPC system with fluorescence lifetime extraction is presented. With optimized hardware and firmware design, the proposed TCSPC system can extract fluorescence lifetime of Fluorescein, Coumarin 6, and Rhodamine 6G down to the concentration of 1 nM, 1nM and 2.5 nM, respectively, demonstrating a new level of performance compared to similar lifetime analysis systems and is suitable for sensing a variety of chemical and biological samples. Methodology in designing compact, portable, integrated TCSPC system opens up the possibility of ubiquitous, rapid, and point-of-care medical diagnostic applications.

REFERENCES

[1] S. Chen, L. Kong, W. Xu, X. Cui, and Q. Liu, "A fast fluorescence background suppression method for Raman spectroscopy based on stepwise spectral reconstruction," *IEEE Access*, vol. 6, pp. 67709–67717, 2018.
[2] X. Dong, C. Chen, and G. Cao, "Improving molecular sensitivity in X-ray fluorescence molecular imaging (XFMI) of iodine distribution in mouse-sized phantoms via excitation spectrum optimization," *IEEE Access*, vol. 6, pp. 56966–56976, 2018.
[3] W. Cong, Y. Xi, and G. Wang, "X-ray fluorescence computed tomography with polycapillary focusing," *IEEE Access*, vol. 2, pp. 1138–1142, 2014.
[4] I. Nissinen, J. Nissinen, P. Keränen, D. Stoppa, and J. Kostamovaara, "A 16 × 256 SPAD line detector with a 50-ps, 3-bit, 256-channel time-to-digital converter for Raman spectroscopy," *IEEE Sensors J.*, vol. 18, no. 9, pp. 3789–3798, Jan. 2018.
[5] D. Tamborini, M. Buttafava, A. Ruggeri, and F. Zappa, "Compact, low-power and fully reconfigurable 10 ps resolution, 160 range, time-resolved single-photon counting system," *IEEE Sensors J.*, vol. 16, no. 10, pp. 3827–3833, May 2016.
[6] D. Ho, M. O. Noor, U. J. Krull, G. Gulak, and R. Genov, "CMOS spectrally-multiplexed FRET-on-a-chip for DNA analysis," *IEEE Trans. Biomed. Circuits Syst.*, vol. 7, no. 5, pp. 643–654, Oct. 2013.
[7] D. Ho, M. O. Noor, U. J. Krull, G. Gulak, and R. Genov, "CMOS tunable-color image sensor with dual-ADC shot-noise-aware dynamic range extension," *IEEE Trans. Circuits Syst. I, Reg. Papers*, vol. 60, no. 8, pp. 2116–2129, Aug. 2013.
[8] D. Ho, M. O. Noor, U. J. Krull, G. Gulak, and R. Genov, "CMOS tunable-wavelength multi-color photogate sensor," *IEEE Trans. Biomed. Circuits Syst.*, vol. 7, no. 6, pp. 805–819, Dec. 2013.
[9] T. A. Abbas, N. A. W. Dutton, O. Almer, N. Finlayson, F. M. D. Rocca, and R. Henderson, "A CMOS SPAD sensor with a multi-event folded flash time-to-digital converter for ultra-fast optical transient capture," *IEEE Sensors J.*, vol. 18, no. 8, pp. 3163–3173, Apr. 2018.
[10] I. Gyongy *et al.*, "A 256×256, 100-kfps, 61% fill-factor SPAD image sensor for time-resolved microscopy applications," *IEEE Trans. Electron Devices*, vol. 65, no. 2, pp. 547–554, Feb. 2018.
[11] M. Y. Berezin and S. Achilefu, "Fluorescence lifetime measurements and biological imaging," *Chem. Rev.*, vol. 110, no. 5, pp. 2641–2684, May 2010.
[12] K. Tanaka *et al.*, "Rational design of fluorescein-based fluorescence probes. Mechanism-based design of a maximum fluorescence probe for singlet oxygen," *J. Amer. Chem. Soc.*, vol. 123, no. 11, pp. 2530–2536, Mar. 2001.
[13] M. Schena, D. Shalon, R. Davis, and P. Brown, "Quantitative monitoring of gene expression patterns with a complementary DNA microarray," *Science*, vol. 270, no. 5235, pp. 467–470, Oct. 1995.
[14] D. I. Kim and K. J. Roux, "Filling the void: Proximity-based labeling of proteins in living cells," *Trends Cell Biol.*, vol. 26, no. 11, pp. 804–817, Nov. 2016.
[15] M. Wichert *et al.*, "Dual-display of small molecules enables the discovery of ligand pairs and facilitates affinity maturation," *Nature Chem.*, vol. 7, no. 3, pp. 241–249, Mar. 2015.
[16] K. Heller, P. Ochtrop, M. F. Albers, F. B. Zauner, A. Itzen, and C. Hedberg, "Covalent protein labeling by enzymatic phosphocholination," *Angewandte Chem. Int. Ed.*, vol. 54, no. 35, pp. 10327–10330, 2015.
[17] X. Zhang *et al.*, "The chemotherapeutic potential of PEG-b-PLGA copolymer micelles that combine chloroquine as autophagy inhibitor and docetaxel as an anti-cancer drug," *Biomaterials*, vol. 35, no. 33, pp. 9144–9154, Nov. 2014.
[18] B. Zhang *et al.*, "Optimization of the tumor microenvironment and nanomedicine properties simultaneously to improve tumor therapy," *Oncotarget*, vol. 7, no. 38, pp. 62607–62618, Aug. 2016.
[19] J. H. Finke, C. Richter, T. Gothsch, A. Kwade, S. Büttgenbach, and C. C. Müller-Goymann, "Coumarin 6 as a fluorescent model drug: How to identify properties of lipid colloidal drug delivery systems via fluorescence spectroscopy?" *Eur. J. Lipid Sci. Technol.*, vol. 116, no. 9, pp. 1234–1246, 2014.
[20] N. Yeredla, T. Kojima, Y. Yang, S. Takayama, and M. Kanapathipillai, "Aqueous two phase system assisted self-assembled PLGA microparticles," *Sci. Rep.*, vol. 6, no. 1, Sep. 2016, Art. no. 27736.
[21] A. Jaworska *et al.*, "Rhodamine 6G conjugated to gold nanoparticles as labels for both SERS and fluorescence studies on live endothelial cells," *Microchim. Acta*, vol. 182, nos. 1–2, pp. 119–127, Jan. 2015.
[22] M. D. Dimitrova, N. I. Georgiev, and V. B. Bojinov, "Novel PAMAM dendron as a bichromophoric probe based on Rhodamine 6G and 1,8-naphthalimide," *J. Fluorescence*, vol. 26, no. 3, pp. 1091–1100, May 2016.
[23] F. Zhang, J. Zhu, J.-J. Li, and J.-W. Zhao, "Fluorescence spectral detection of cysteine based on the different medium-coated gold nanorods-Rhodamine 6G probe: From quenching to enhancement," *Sens. Actuators B, Chem.*, vol. 220, pp. 1279–1287, Dec. 2015.
[24] Y. Fu *et al.*, "A new fluorescent probe for Al 3+ based on rhodamine 6G and its application to bioimaging," *Dalton Trans.*, vol. 43, no. 33, pp. 12624–12632, Jun. 2014.

[25] Q. Liu *et al.*, "A highly sensitive SERS method for the determination of nitrogen oxide in air based on the signal amplification effect of nitrite catalyzing the bromate oxidization of a rhodamine 6G probe," *RSC Adv.*, vol. 4, no. 21, pp. 10955–10959, 2014.

[26] Y. He and L. Geng, "Phase-sensitive fluorescence lifetime detection in capillary electrophoresis," *Anal. Chem.*, vol. 73, no. 5, pp. 943–950, Mar. 2001.

[27] W. Becker, *Advanced Time-Correlated Single Photon Counting Techniques*. Berlin, Germany: Springer, 2005.

[28] J. Kissinger and D. Wilson, "Portable fluorescence lifetime detection for chlorophyll analysis in marine environments," *IEEE Sensors J.*, vol. 11, no. 2, pp. 288–295, Feb. 2011.

[29] D. Phillips, R. C. Drake, D. V. O'Connor, and R. L. Christensen, "Time correlated single-photon counting (TCSPC) using laser excitation," *Instrum. Sci. Technol.*, vol. 14, nos. 3–4, pp. 267–292, Jan. 1985.

[30] R. E. Connally and J. A. Piper, "Time-gated luminescence microscopy," *Ann. New York Acad. Sci.*, vol. 1130, no. 1, pp. 106–116, May 2008.

[31] A. D. Mora *et al.*, "Fast-gated single-photon avalanche diode for wide dynamic range near infrared spectroscopy," *IEEE J. Sel. Topics Quantum Electron.*, vol. 16, no. 4, pp. 1023–1030, Jul. 2010.

[32] W. Becker, "Fluorescence lifetime imaging–techniques and applications," *J. Microsc.*, vol. 247, no. 2, pp. 119–136, Aug. 2012.

[33] B. R. Rae *et al.*, "A vertically integrated CMOS microsystem for time-resolved fluorescence analysis," *IEEE Trans. Biomed. Circuits Syst.*, vol. 4, no. 6, pp. 437–444, Dec. 2010.

[34] H. Wang, Y. Qi, T. J. Mountziaris, and C. D. Salthouse, "A portable time-domain LED fluorimeter for nanosecond fluorescence lifetime measurements," *Rev. Sci. Instrum.*, vol. 85, no. 5, p. 055003, 2014.

[35] D. C. Lamb, B. K. Müller, and C. Bräuchle, "Enhancing the sensitivity of fluorescence correlation spectroscopy by using time-correlated single photon counting," *Current Pharmaceutical Biotechnol.*, vol. 6, no. 5, pp. 405–414, Oct. 2005.

[36] W. Becker, "Fluorescence lifetime imaging by multi-dimensional time correlated single photon counting," *Med. Photon.*, vol. 27, pp. 41–61, May 2015.

[37] W. Becker, A. Bergmann, M. A. Hink, K. König, K. Benndorf, and C. Biskup, "Fluorescence lifetime imaging by time-correlated single-photon counting," *Microsc. Res. Techn.*, vol. 63, no. 1, pp. 58–66, Jan. 2004.

[38] C. Y. Fu, B.-K. Ng, and S. G. Razul, "Fluorescence lifetime discrimination using expectation-maximization algorithm with joint deconvolution," *J. Biomed. Opt.*, vol. 14, no. 6, 2009, Art. no. 064009.

[39] S. Antonioli, L. Miari, A. Cuccato, M. Crotti, I. Rech, and M. Ghioni, "8-channel acquisition system for time-correlated single-photon counting," *Rev. Sci. Instrum.*, vol. 84, no. 6, Jun. 2013, Art. no. 064705.

[40] B. Markovic, S. Tisa, F. A. Villa, A. Tosi, and F. Zappa, "A high-linearity, 17 ps precision time-to-digital converter based on a single-stage Vernier delay loop fine interpolation," *IEEE Trans. Circuits Syst. I, Reg. Papers*, vol. 60, no. 3, pp. 557–569, Mar. 2013.

[41] M. Kanoun, M. W. Ben Attouch, Y. Bérubé-Lauzière, and R. Fontaine, "A 10-bit, 12 ps resolution CMOS time-to-digital converter dedicated to ultra-fast optical timing applications," *Circuits, Syst., Signal Process.*, vol. 34, no. 4, pp. 1129–1148, Apr. 2015.

[42] D. Tamborini, B. Markovic, F. Villa, and A. Tosi, "16-channel module based on a monolithic array of single-photon detectors and 10-ps time-to-digital converters," *IEEE J. Sel. Topics Quantum Electron.*, vol. 20, no. 6, pp. 218–225, Nov. 2014.

[43] D. Tamborini, D. Portaluppi, F. Villa, and F. Zappa, "Eight-channel 21 ps precision 10 μs range time-to-digital converter module," *IEEE Trans. Instrum. Meas.*, vol. 65, no. 2, pp. 423–430, Feb. 2016.

[44] N. Roy, F. Nolet, F. Dubois, M.-O. Mercier, R. Fontaine, and J.-F. Pratte, "Low power and small area, 6.9 ps RMS time-to-digital converter for 3-D digital SiPM," *IEEE Trans. Radiat. Plasma Med. Sci.*, vol. 1, no. 6, pp. 486–494, Nov. 2017.

[45] T. F. da Silva, G. B. Xavier, and J. P. von der Weid, "Real-time characterization of gated-mode single-photon detectors," *IEEE J. Quantum Electron.*, vol. 47, no. 9, pp. 1251–1256, Sep. 2011.

[46] D. Portaluppi, E. Conca, and F. Villa, "32×32 CMOS SPAD imager for gated imaging, photon timing, and photon coincidence," *IEEE J. Sel. Topics Quantum Electron.*, vol. 24, no. 2, Mar./Apr. 2018, Art. no. 3800706.

[47] I. Nissinen, J. Nissinen, P. Keranen, A.-K. Lansman, J. Holma, and J. Kostamovaara, "A 2×(4)×128 multitime-gated SPAD line detector for pulsed Raman spectroscopy," *IEEE Sensors J.*, vol. 15, no. 3, pp. 1358–1365, Mar. 2015.

[48] M. Perenzoni, N. Massari, D. Perenzoni, L. Gasparini, and D. Stoppa, "A 160×120 pixel analog-counting single-photon imager with time-gating and self-referenced column-parallel A/D conversion for fluorescence lifetime imaging," *IEEE J. Solid-State Circuits*, vol. 51, no. 1, pp. 155–167, Jan. 2016.

[49] F. Villa, R. Lussana, D. Tamborini, A. Tosi, and F. Zappa, "High-fill-factor 60×1 SPAD array with 60 subnanosecond integrated TDCs," *IEEE Photon. Technol. Lett.*, vol. 27, no. 12, pp. 1261–1264, Jun. 15, 2015.

[50] M. Sanzaro, P. Gattari, F. Villa, A. Tosi, G. Croce, and F. Zappa, "Single-photon avalanche diodes in a 0.16 μm BCD technology with sharp timing response and red-enhanced sensitivity," *IEEE J. Sel. Topics Quantum Electron.*, vol. 24, no. 2, Mar./Apr. 2018, Art. no. 3801209.

[51] H. Wang, Y. Yang, Z. Huang, and H. Gui, "Instrument for real-time measurement of low turbidity by using time-correlated single photon counting technique," *IEEE Trans. Instrum. Meas.*, vol. 64, no. 4, pp. 1075–1083, Apr. 2015.

[52] S. Antonioli, M. Crotti, A. Cuccato, I. Rech, and M. Ghioni, "Time-correlated single-photon counting system based on a monolithic time-to-amplitude converter," *J. Mod. Opt.*, vol. 59, no. 17, pp. 1512–1524, Oct. 2012.

[53] A. Cuccato *et al.*, "Complete and compact 32-channel system for time-correlated single-photon counting measurements," *IEEE Photon. J.*, vol. 5, no. 5, p. 6801514, Oct. 2013.

[54] Y. Wang *et al.*, "Ultra-portable explosives sensor based on a CMOS fluorescence lifetime analysis micro-system," *AIP Adv.*, vol. 1, no. 3, Sep. 2011, Art. no. 032115.

[55] B. R. Rae *et al.*, "A CMOS time-resolved fluorescence lifetime analysis micro-system," *Sensors*, vol. 9, no. 11, pp. 9255–9274, Nov. 2009.

[56] J. Bouchard *et al.*, "A low-cost time-correlated single photon counting system for multiview time-domain diffuse optical tomography," *IEEE Trans. Instrum. Meas.*, vol. 66, no. 10, pp. 2505–2515, Oct. 2017.

[57] D. Tyndall *et al.*, "A high-throughput time-resolved mini-silicon photomultiplier with embedded fluorescence lifetime estimation in 0.13 μm CMOS," *IEEE Trans. Biomed. Circuits Syst.*, vol. 6, no. 6, pp. 562–570, Dec. 2012.

[58] R. M. Field, S. Realov, and K. L. Shepard, "A 100 fps, time-correlated single-photon-counting-based fluorescence-lifetime imager in 130 nm CMOS," *IEEE J. Solid-State Circuits*, vol. 49, no. 4, pp. 867–880, Apr. 2014.

[59] M. G. Badea and L. Brand, "Time-resolved fluorescence measurements," in *Methods in Enzymology*, vol. 61. San Diego, CA, USA: Elsevier, 1979, pp. 378–425.

[60] A. Grinvald and I. Z. Steinberg, "On the analysis of fluorescence decay kinetics by the method of least-squares," *Anal. Biochem.*, vol. 59, no. 2, pp. 583–598, Jun. 1974.

[61] W. R. Ware, L. J. Doemeny, and T. L. Nemzek, "Deconvolution of fluorescence and phosphorescence decay curves. Least-squares method," *J. Phys. Chem.*, vol. 77, no. 17, pp. 2038–2048, 1973.

[62] C. Liu, Y. Zhou, X. Wang, and Y. Liu, "Lifetime computing algorithms based on exponential pattern retrieve and polynomial fitting in fluorescence lifetime imaging microscopy," presented at the Int. Conf. Opt. Instrum. Technol., Optoelectron. Imag. Process. Technol., vol. 8200, 2011, p. 82000X.

[63] C. Liu, X. Wang, Y. Zhou, and Y. Liu, "Timing and operating mode design for time-gated fluorescence lifetime imaging microscopy," *Sci. World J.*, vol. 2013, Jun. 2013, Art. no. 801901.

[64] D. V. O'Connor, *Time-correlated Single Photon Counting*. New York, NY, USA: Academic, 2012.

[65] J. R. Lakowicz, Ed., "Time-domain lifetime measurements," in *Principles of Fluorescence Spectroscopy*. New York, NY, USA: Springer, 2006, pp. 97–155.

[66] J. Léonard *et al.*, "High-throughput time-correlated single photon counting," *Lab. Chip*, vol. 14, no. 22, pp. 4338–4343, Oct. 2014.

[67] S. Preus, "Spectroscopic tools for quantitative studies of dna structure and dynamics," Ph.D. dissertation, Dept. Chem., Fac. Sci., Univ. Copenhagen, Copenhagen, Denmark, 2012.

[68] J. C. Lagarias, J. A. Reeds, M. H. Wright, and P. E. Wright, "Convergence properties of the Nelder-Mead simplex method in low dimensions," *SIAM J. Optim.*, vol. 9, no. 1, pp. 112–147, 1998.

[69] J. R. Lakowicz, Ed., "Instrumentation for fluorescence spectroscopy," in *Principles of Fluorescence Spectroscopy*. New York, NY, USA: Springer, 2006, pp. 27–61.

[70] T. Bernas, J. P. Robinson, E. K. Asem, and B. Rajwa, "Loss of image quality in photobleaching during microscopic imaging of fluorescent probes bound to chromatin," *J. Biomed. Opt.*, vol. 10, no. 6, 2005, Art. no. 064015.
[71] W. Harm, *Biological Effects of Ultraviolet Radiation* (IUPAB Biophysics Series), 1st ed. Cambridge, U.K.: Cambridge Univ. Press, 1980, pp. 23–73.
[72] P. Kapusta, Ed., *Advanced Photon Counting: Applications, Methods, Instrumentation*. Cham, Switzerland: Springer, 2015.
[73] S. Donati and T. Tambosso, "Single-photon detectors: From traditional PMT to solid-state spad-based technology," *IEEE J. Sel. Topics Quantum Electron.*, vol. 20, no. 6, pp. 204–211, Nov. 2014.
[74] M. W. Fishburn and E. Charbon, "System tradeoffs in gamma-ray detection utilizing SPAD arrays and scintillators," *IEEE Trans. Nucl. Sci.*, vol. 57, no. 5, pp. 2549–2557, Oct. 2010.
[75] A. Tosi *et al.*, "Fast-gated single-photon counting technique widens dynamic range and speeds up acquisition time in time-resolved measurements," *Opt. Express*, vol. 19, no. 11, pp. 10735–10746, May 2011.
[76] A. Kechkar, D. Nair, M. Heilemann, D. Choquet, and J.-B. Sibarita, "Real-time analysis and visualization for single-molecule based super-resolution microscopy," *PLoS ONE*, vol. 8, no. 4, Apr. 2013, Art. no. e62918.
[77] J. Ferreira, "Modular textile-enabled bioimpedance system for personalized health monitoring applications," Ph.D. dissertation, School Technol. Health, KTH Roy. Inst. Technol., Stockholm, Sweden, 2017.
[78] S. Cova and M. Bertolaccini, "Differential linearity testing and precision calibration of multichannel time sorters," *Nucl. Instrum. Methods*, vol. 77, no. 2, pp. 269–276, Jan. 1970.
[79] P. Jani, L. Vámos, and T. Nemes, "Timing resolution (FWHM) of some photon counting detectors and electronic circuitry," *Meas. Sci. Technol.*, vol. 18, no. 1, pp. 155–160, Jan. 2007.
[80] G. B. Dutt, G. R. Krishna, and S. Raman, "Rotational dynamics of coumarins in nonassociative solvents: Point dipole versus extended charge distribution models of dielectric friction," *J. Chem. Phys.*, vol. 115, no. 10, pp. 4732–4741, Sep. 2001.

YI TIAN received the B.A.Sc. degree in electronics information science and technology and the M.A.Sc. degree in circuit and system from Lanzhou University, Lanzhou, China, in 2010 and 2013, respectively. He is currently pursuing the Ph.D. degree in materials science and engineering with the City University of Hong Kong, Hong Kong. His research interest includes the development of compact time-correlated single photon counting lifetime analytical systems.

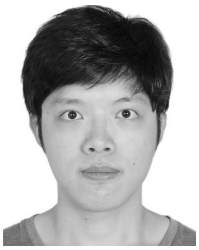

WENRONG YAN received the B.Eng. degree in material science and engineering from the South China University of Technology, Guangzhou, China, in 2013. He is currently pursuing the Ph.D. degree in materials science and engineering with the City University of Hong Kong, Hong Kong. His research focuses on graphene-based soft sensor and energy device for wearable application.

LIPING WEI received the B.A.Sc. degree in electronic science and technology and the M.A.Sc. degree in technology and instrument of test and measurement from the North University of China, China, in 2011 and 2014, respectively. She is currently pursuing the Ph.D. degree in materials science and engineering with the City University of Hong Kong, Hong Kong. Her research focuses on developing compact time-correlated single photon counting fluorescence lifetime measurement systems for biological applications.

DEREK HO received the Ph.D. degree from the Department of Electrical and Computer Engineering, University of Toronto, Toronto, Canada, in 2013. He is currently an Assistant Professor with the Department of Materials Science and Engineering, City University of Hong Kong. His researches incorporate the synthesis of nanostructured materials, device optimization, and microsystem integration for applications in chemical, physical, and biological sensors. He is a member of the IEEE Biomedical and Life Science Circuits and Systems Technical Committee. He was a co-recipient of the Championship of the IEEE International Microwave Symposium Student Design Competition, in 2017.